Article

Molecular Cell

Monoubiquitination of Histone H2B Blocks Eviction of Histone Variant H2A.Z from Inducible Enhancers

Graphical Abstract

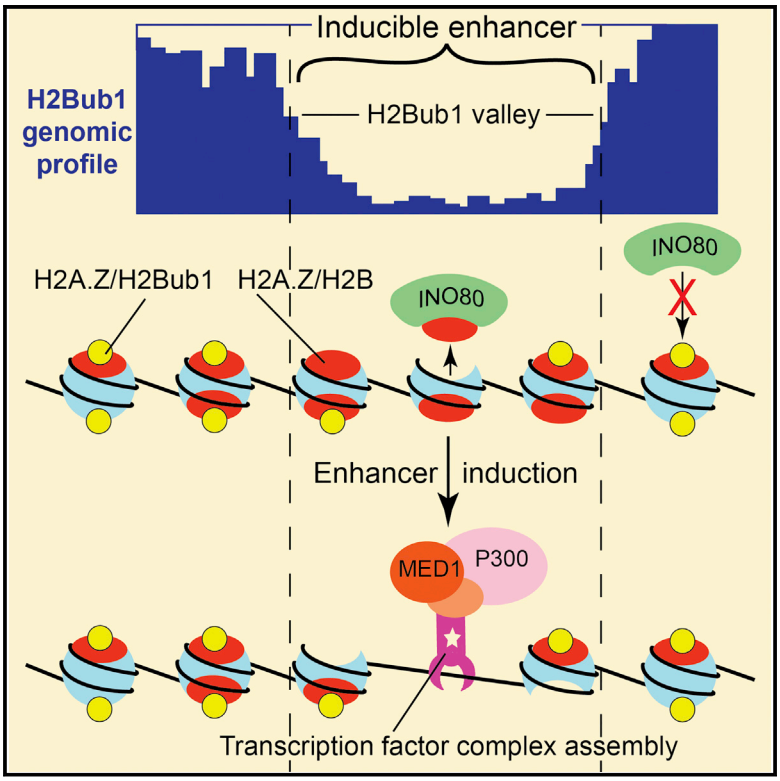

Authors

Gregory Segala, Marcela A. Bennesch, Deo Prakash Pandey, Nicolas Hulo, Didier Picard

Correspondence

didier.picard@unige.ch

In Brief

Monoubiquitinated histone H2B (H2Bub1) promotes transcription elongation, but whether it regulates other aspects of gene expression is unclear. Segala et al. show that H2Bub1 limits chromatin accessibility and transcription factor binding at inducible enhancers and propose that it negatively regulates the exchange of the histone variant H2A.Z.

Highlights

- Monoubiquitination of histone H2B (H2Bub1) represses inducible enhancers
- At the center of inducible enhancers, H2Bub1 levels decrease to form H2Bub1 valleys
- The histone variant H2A.Z is stabilized by H2Bub1 at inducible enhancers
- H2Bub1 impairs chromatin access to INO80, an H2A.Z evictor

Segala et al., 2016, Molecular Cell *64*, 334–346
October 20, 2016
http://dx.doi.org/10.1016/j.molcel.2016.08.034

CellPress

CellPress

Molecular Cell
Article

Monoubiquitination of Histone H2B Blocks Eviction of Histone Variant H2A.Z from Inducible Enhancers

Gregory Segala,[1,2] Marcela A. Bennesch,[1,2] Deo Prakash Pandey,[1,3] Nicolas Hulo,[2] and Didier Picard[1,2,4,*]
[1]Département de Biologie Cellulaire
[2]Institute of Genetics and Genomics of Geneva
Université de Genève, 1211 Genève 4, Switzerland
[3]Present address: Biotech Research and Innovation Center, University of Copenhagen, 2200 Copenhagen, Denmark
[4]Lead Contact
*Correspondence: didier.picard@unige.ch
http://dx.doi.org/10.1016/j.molcel.2016.08.034

SUMMARY

Covalent modifications of histones play a crucial role in the regulation of gene expression. Histone H2B monoubiquitination has mainly been described as a regulator of transcription elongation, but its role in transcription initiation is poorly documented. We investigated the role of this histone mark (H2Bub1) on different inducible enhancers, in particular those regulated by estrogen receptor α, by loss- and gain-of-function experiments with the specific E3-ubiquitin ligase complex of H2B: RNF20/RNF40. RNF20/RNF40 overexpression causes repression of the induced activity of these enhancers. Genome-wide profiles show that H2Bub1 levels are negatively correlated with the accessibility of enhancers to transcriptional activators. We found that the chromatin association of histone variant H2A.Z, which is evicted from enhancers for transcriptional activation, is stabilized by H2Bub1 by impairing access of the chromatin remodeler INO80. We propose that H2Bub1 acts as a gatekeeper of H2A.Z eviction and activation of inducible enhancers.

INTRODUCTION

In eukaryotes, gene expression is challenged by the fact that DNA is wrapped around nucleosomes, which imposes a physical constraint for the access of transcription factors and RNA polymerases to DNA (Teves et al., 2014). Some regulatory regions of the genome, including enhancers, insulators, and promoters, need to be partly accessible to transacting factors to allow the regulation and adaptation of gene expression. Post-translational modifications of histones and the replacement of histones by histone variants have emerged as the central mechanisms by which cells regulate the stability of the nucleosomes at defined regions of the genome (Venkatesh and Workman, 2015). Post-translational modifications of histones can have activator or repressive roles for gene expression by affecting chromatin accessibility (Zentner and Henikoff, 2013).

H2B monoubiquitination (H2Bub1) is a conserved histone mark present in fungi, plants, and mammals (Weake and Workman, 2008), indicating an essential role in eukaryotes. In mammals, the heterodimeric proteins RNF20/RNF40 are the specific E3-ubiquitin ligases for H2B (Zhu et al., 2005). H2Bub1 was found to decrease strongly in primary tumor samples of late-stage breast cancer, suggesting a tumor suppressor role of H2Bub1 (Prenzel et al., 2011). In line with this hypothesis, estrogen-dependent breast cancer cells are able to proliferate without estrogen when RNF40 is knocked down (Prenzel et al., 2011). Surprisingly, the inactivation of RNF20/40 has only a moderate effect on overall gene expression levels (Shema et al., 2008), raising the possibility that the H2Bub1 chromatin mark could be dedicated to the regulation of specific groups of genes rather than the regulation of the whole genome. Indeed, H2Bub1 has been associated with the regulation of inducible genes involved in cell differentiation (Zhu et al., 2005; Fuchs et al., 2012; Karpiuk et al., 2012; Materne et al., 2016) and inflammation (Tarcic et al., 2016), suggesting a role for H2Bub1 in the regulation of inducible rather than constitutive transcription. Genomic analyses showed that H2Bub1 is enriched in actively transcribed regions of human genes (Minsky et al., 2008), and it has been proposed to be involved in the regulation of global transcriptional elongation (Pavri et al., 2006; Minsky et al., 2008). In support of this notion, it was shown that H2B monoubiquitination regulates nucleosome reassembly during transcriptional elongation (Fleming et al., 2008) and that the co-transcriptional monoubiquitination of H2B is tightly coupled with the elongation rate of RNA polymerase II (Fuchs et al., 2014). Interestingly, it has been pointed out that H2Bub1 could be an activator in transcribed regions while having a repressive function in promoters (Batta et al., 2011; Materne et al., 2016), but the underlying molecular mechanisms have not been studied in mammalian cells. These preliminary observations raise the possibility that H2Bub1 could be involved in regulating transcription initiation, which might explain why H2Bub1 depletion could have gene-specific effects. This speculation is further supported by the fact that the H2B deubiquitinase USP22 is part of the coactivator complex Spt-Ada-Gcn5 acetyltransferase (SAGA) and is required for the activation of transcription (Zhang et al., 2008).

Transcription initiation is strongly regulated by genetic elements called enhancers. Enhancers contain DNA motifs that are recognized by specific transcription factors. These transcription

factors, their co-regulators, and the chromatin organization determine when and where these enhancers will be active to stimulate the transcription of their target genes (Shlyueva et al., 2014). The composition of the chromatin of regulatory elements is enriched by specific histone marks and some histone variants. Several histone marks, like H3K27ac or H3K27me3, which regulate positive or negative gene expression, respectively, define the activity of enhancers (Shlyueva et al., 2014). The histone variants H2A.Z and H3.3 are incorporated at the level of regulatory elements such as enhancers and promoters. Nucleosomes containing these two variants are particularly unstable (Jin et al., 2009), which makes these chromatin regions dynamic and more easily accessible to transacting factors. The histone variant H2A.Z was described as an essential determinant of the inducible transcriptional activation mediated by the estrogen receptor α (ERα) (Gévry et al., 2009; Brunelle et al., 2015). Despite its positive role for gene activation, it was found that H2A.Z dissociates from enhancers during inducible gene activation (Gévry et al., 2009; Chauhan and Boyd, 2012), maybe in the course of nucleosome disassembly (Papamichos-Chronakis et al., 2011; Yen et al., 2013). Importantly, there could be a crosstalk between histone modifications and H2A.Z dynamics; it was reported that H2A.Z distribution across the genome can be controlled by H3K56ac and that this alters the deposition of H2A.Z by the Swr1 complex (SWR-C) remodeling enzyme (Watanabe et al., 2013).

Despite considerable progress in the last few decades, the chromatin features at inducible enhancers that allow and promote rapid and reversible activation are still incompletely understood. Considering the possibility that H2Bub1 could be involved in regulating transcription initiation, we decided to explore the hypothesis that H2Bub1 regulates inducible rather than constitutive enhancers by using the transcriptional regulation by nuclear receptors such as ERα as a model system. These ligand-activatable transcription factors rapidly trigger the activation of specific inducible enhancers in response to their cognate ligand. This affords the unique opportunity to explore chromatin determinants of inducible enhancers very easily before and after activation.

RESULTS

RNF20/40 Repress Inducible Enhancers

We performed experiments with a panel of luciferase reporter gene constructs controlled by ERα (induced by 17β-estradiol [E2]), the progesterone receptor (PR) (induced by progesterone [P4]), or the glucocorticoid receptor (GR) (induced by dexamethasone [Dex]) transfected into human HEK293T cells (Figures 1A–1D and S1A, available online). Overexpression of RNF20 or RNF40 and especially their concomitant overexpression inhibited the induction of these enhancers without significant effects on their basal levels. This inhibitory effect depends on the presence of an inducible enhancer because a construct devoid of any enhancer is not sensitive to the effect of RNF20/40 (Figure 1E). Conversely, we confirmed that RNF20/40 repress enhancer activity by knockdown experiments with two different short hairpin RNAs (shRNAs) each (Figures 1F and S1B–S1G). This repressive effect is independent of cell context because it could also be observed with breast and lung cancer cells (Figures 1G, S1H, and S1I). The levels of the corresponding transcription factor, ERα, were not affected by RNF20/40 knockdown or overexpression, whereas corresponding changes could be seen for the H2Bub1 levels (Figures 1H and S1J). Our results mirrored the fact that RNF20/40 function as a heterodimer (Zhu et al., 2005; Pavri et al., 2006) because the combined overexpression was more efficient (Figure S1J), and knockdown of either one, as reported previously (Pavri et al., 2006), was as efficient as their combined knockdown (Figure 1H). To corroborate further that RNF20/40 specifically act on inducible enhancers, we used chimeras consisting of the Gal4 DNA binding domain fused to either the N-terminal or the ligand binding domains of ERα, which are responsible for its constitutive or inducible transactivation activities, respectively (Bennesch and Picard, 2015). Only the inducible chimeric transcription factor proved to be affected by RNF20/40 (Figures 1I and 1J). Overexpression of H2B by itself repressed the enhancer activity and impaired the repression by RNF20/40, perhaps by flooding cells with an excess of H2B. In comparison with wild-type H2B, overexpression of the H2B monoubiquitination mutant K120R recapitulated the de-repressive effect of the knockdown of RNF20/40 (Figure 1K). Parallel experiments with the proteasome inhibitor MG132 supported the conclusion that RNF20/40 repress inducible enhancers through the monoubiquitination of H2B independent of proteasomal degradation (Figure S1K).

RNF20/40 Inhibit Endogenous ERα Target Gene Expression by Repressing Inducible Enhancers

We then examined the role of RNF20/40 for the regulation of endogenous ERα target genes in MDA-MB134 breast cancer cells, which we have used interchangeably with MCF-7 cells. Knockdown of RNF20/40 stimulated the E2-induced expression of a panel of ERα target genes (Figures 2A–2F). To assess more directly the activity of the enhancers that regulate the expression of the two ERα target genes *GREB1* and *TFF1*, we measured the production of the associated enhancer RNAs (eRNAs), which are transcribed in both orientations (Li et al., 2013). The activities of the enhancers of *GREB1* and *TFF1* are stimulated by knockdown of RNF20/40, and this correlates with an increase in the recruitment of ERα and the pioneer factor FOXA1 (Hurtado et al., 2011) to these enhancers (Figures 2G–2L, S2B, and S2C), without any change of the total FOXA1 protein levels (Figure S2A). These results suggest that RNF20/40 repress inducible enhancers by decreasing the recruitment of key transcription factors, possibly as a result of shaping the chromatin environment around these enhancers.

H2Bub1 Is Depleted from the Core of Inducible Enhancers and Open Chromatin

We therefore explored the genome-wide chromatin immunoprecipitation sequencing (ChIP-seq) profiles of H2Bub1, ERα, the coactivators Med1 and P300, and chromatin accessibility (DNase sequencing) using publicly available datasets (He et al., 2012; Liu et al., 2014; Nagarajan et al., 2014) for MCF-7 breast cancer cells (Figure 3A). As expected, H2Bub1 is increased across the ERα target genes *GREB1* and *TFF1* upon induction by E2. However, at the level of the inducible enhancers, characterized by the co-localization of ERα, Med1, P300, and DNase hypersensitive sites (DHSs), the relative levels of H2Bub1 display

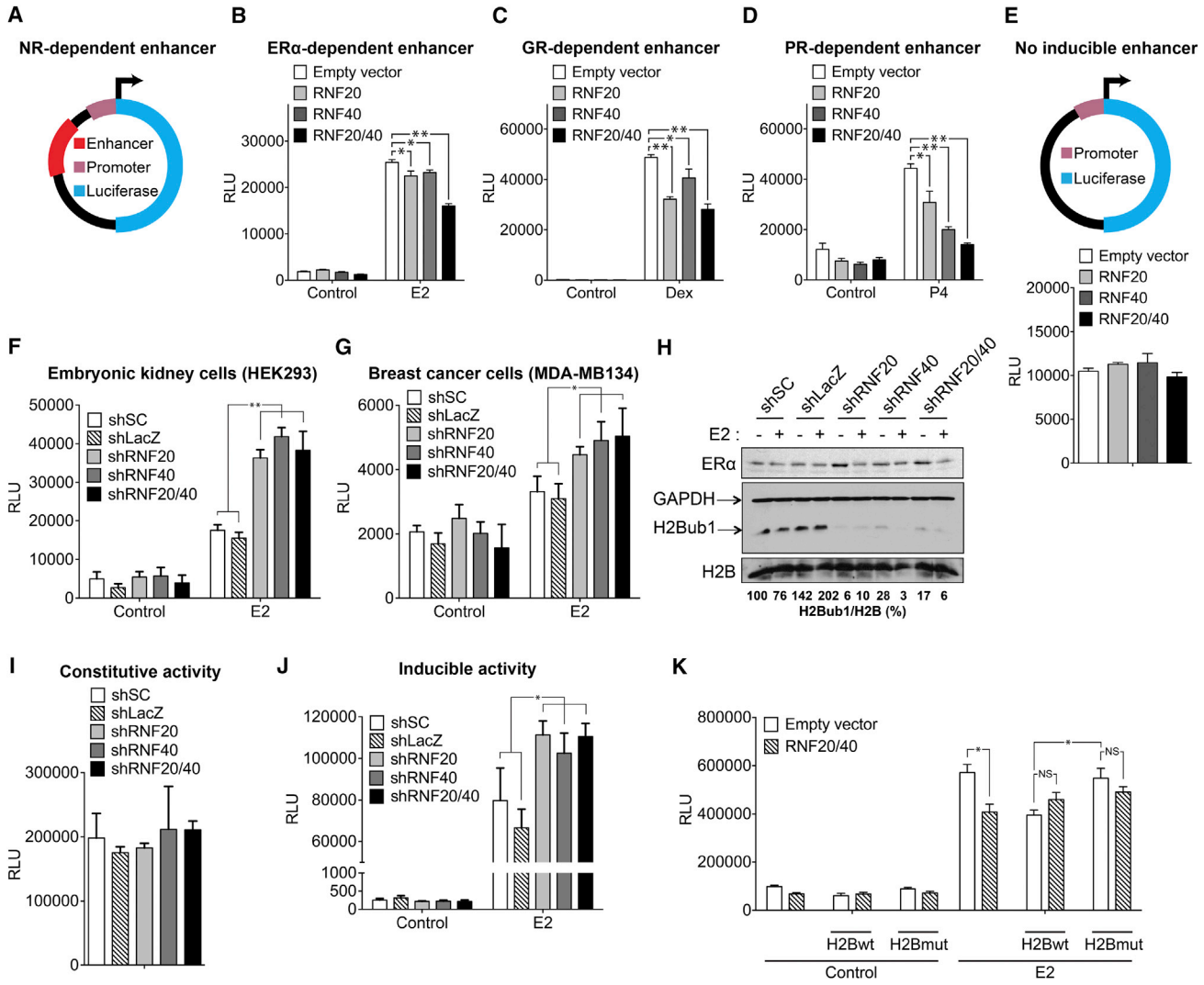

Figure 1. The H2B Monoubiquitination Enzymes RNF20/RNF40 Downregulate Inducible Transcriptional Activity through Enhancer Regulation

(A) Schematic of the luciferase reporter constructs used for the experiments shown in (B)–(D), (F), and (G).

(B–E) Luciferase reporter assays in HEK293T cells with (B–D) or without (E, bottom) the corresponding nuclear receptor-dependent enhancer constructs upon overexpression of RNF20, RNF40, or both. Cells were treated with vehicle alone (Control) or with E2 (B), Dex (C), or (D).

(F and G) Luciferase reporter gene assays with the ERα-dependent enhancer construct in HEK293T (F) or breast cancer cells (MDA-MB134) (G) infected with lentiviral shRNA constructs against RNF20, RNF40, or both. A scrambled shRNA (shSC) and an shRNA targeting the bacterial β-galactosidase (shLacZ) were used as negative controls.

(H) Immunoblot showing the levels of ERα protein and monoubiquitination of histone H2B (H2Bub1) in MDA-MB134 cells infected with the indicated shRNA constructs. The H2Bub1/H2B ratios indicated below the image were determined with the software ImageJ.

(I and J) Luciferase reporter assays with a Gal4-dependent enhancer construct in HEK293T cells infected with the indicated shRNA constructs. Chimeric proteins with the Gal4 DNA binding domain fused to the N-terminal domain of ERα carrying the constitutively active activation function 1 (I) or to the ligand binding domain of ERα with the ligand-inducible activation function 2 (J) were used to assess the effect of H2B monoubiquitination on constitutive or inducible transcriptional activity, respectively.

(K) Luciferase reporter assays with an ERα-dependent enhancer in HEK293T cells overexpressing FLAG-tagged RNF20 and RNF40 along with wild-type H2B (H2Bwt) or the H2B mutant K120/125R (H2Bmut).

(B–G and I–K) RLU, relative luciferase units. Relevant statistically significant values, determined as indicated in the Experimental Procedures, are highlighted by asterisks (*$p < 0.01$, **$p < 0.0001$). An empty vector was transfected as a negative control for overexpression experiments.

The bar graphs show averages of several independent experiments with technical replicates and the errors of the means. See also Figures S1A–S1K.

a drastic drop. We then grouped the ERα binding sites (ERBSs) according to their strength and observed that the H2Bub1 signal across the ERBS is proportional to the strength of the ERBS. Interestingly, there is a relative drop of H2Bub1 levels, hereafter referred to as an "H2Bub1 valley," at the center of high ERBSs independent of any induction (Figures 3B–3D). To ascertain

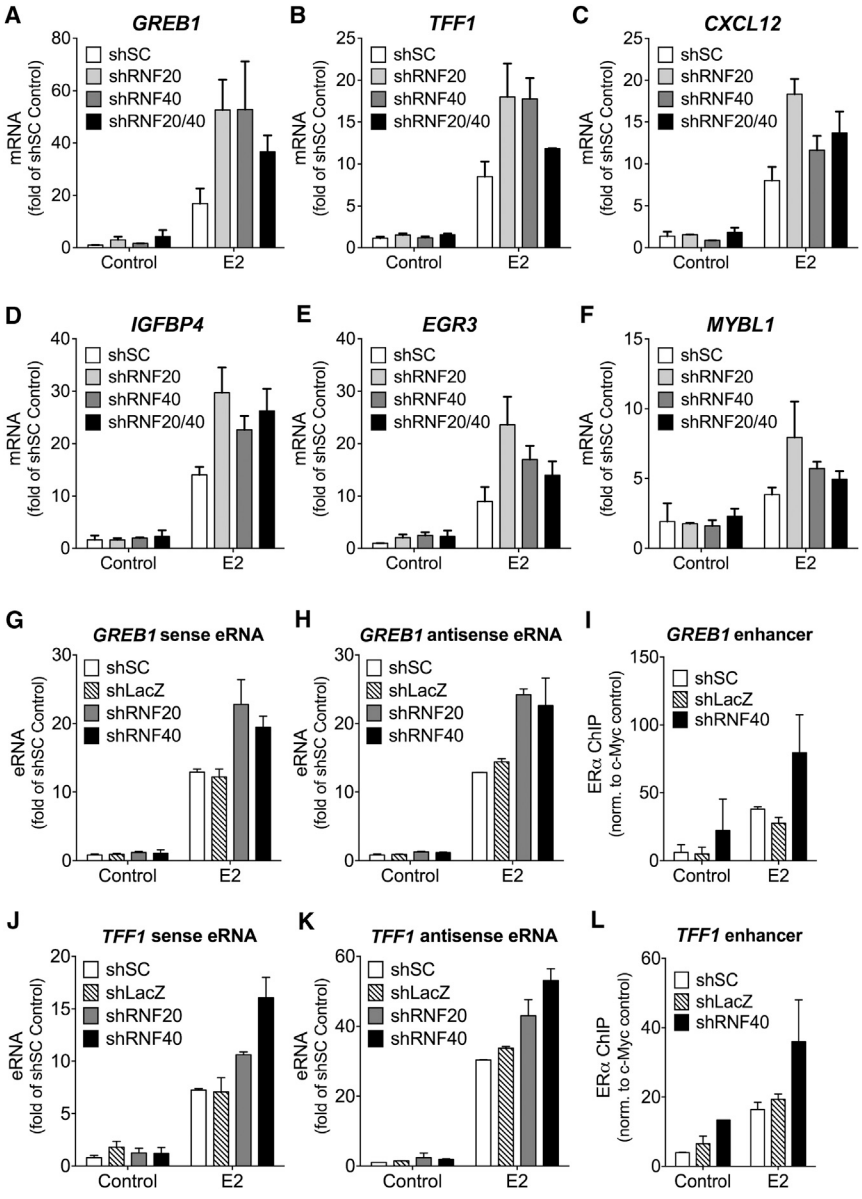

Figure 2. Impairment of Histone H2B Monoubiquitination Increases Endogenous Enhancer Activity and Target Gene Expression

(A–F) qPCR quantification of the expression of ERα target genes in MDA-MB134 cells infected with shRNA constructs as indicated. mRNA levels are expressed relative to the shSC control condition.

(G, H, J, and K) Quantification by qPCR of the eRNAs of the *GREB1* (G and H) and *TFF1* (J and K) enhancers in shRNA-infected MDA-MB134 cells. eRNA levels are expressed relative to the shSC control condition.

(I and L) ChIP-qPCR of ERα on the *GREB1* (I) and *TFF1* (L) enhancers in shRNA-infected MDA-MB134 cells. ERα ChIP-qPCR values are standardized to the first intron of *c-MYC*.

The bar graphs show averages of several independent experiments with technical replicates and the errors of the means. See also Figures S2A–S2C.

that these valleys genuinely exist relative to total H2B bound at these sites, we had to resort to a higher-resolution method. We closely examined the relative levels of H2Bub1 over H2B at the *GREB1* and *TFF1* enhancers at nucleosomal resolution by digesting chromatin with micrococcal nuclease (MNase) for ChIP assays. Again, H2Bub1 valleys could clearly be seen at the centers of these enhancers, even upon standardizing to total H2B (Figure S3A). Induction by E2 further accentuates H2Bub1 valleys in a statistically significant fashion at the center of high ERBSs, whereas a peak of H2Bub1 is observed for low ERBSs and the combination of all types of ERBSs (Figures 3C, 3D, and S3B). A kinetic analysis by ChIP of the H2Bub1/H2B ratio at the centers of the *GREB1* and *TFF1* enhancers showed that H2Bub1 levels drop strongly by 30 min following induction by E2 and that low levels are maintained thereafter (Figure 3E), further supporting the genome-wide data.

Importantly, pronounced H2Bub1 valleys coincide with several other hallmarks of active enhancers and regulatory sequences, including Med1 and P300 binding, DHS, and transcription start sites (TSSs) (Figures 3F–3H and S3C). This implied that H2Bub1 valleys are more generally associated with active enhancers and chromatin regions that need to be accessible to regulatory factors. To clarify this issue, we called the broad peaks of H2Bub1 and bioinformatically extracted the gaps between the peaks as valleys (Figures S3D and S3E). We observed roughly opposite profiles of chromatin accessibility and nucleosome occupancy for H2Bub1 peaks and H2Bub1 valleys, which suggested an involvement of H2Bub1 in nucleosome stabilization (Figures 3I and 3J), as proposed previously (Chandrasekharan et al., 2009). Repressive histone marks like H3K9me3 and H3K27me3 are decreased in H2Bub1 valleys but increased in H2Bub1 peaks, whereas it is exactly the opposite for the active enhancer mark H3K27ac (Figures S3F–S3I). Even when the induction by E2 modifies the intensity of the signals, the profiles are independent of any induction, consistent with the idea that the chromatin environment is already preset before induction. H2Bub1 levels seem to be specific to enhancer-related histone marks because no clear profile was observed for the insulator factor CCCTC-binding factor (CTCF) (Figure S3J). These results demonstrated that regions comprising highly inducible enhancers are characterized by high levels of H2Bub1 that drop at the level of the transcriptional activator binding sites, presumably to increase chromatin accessibility to these factors.

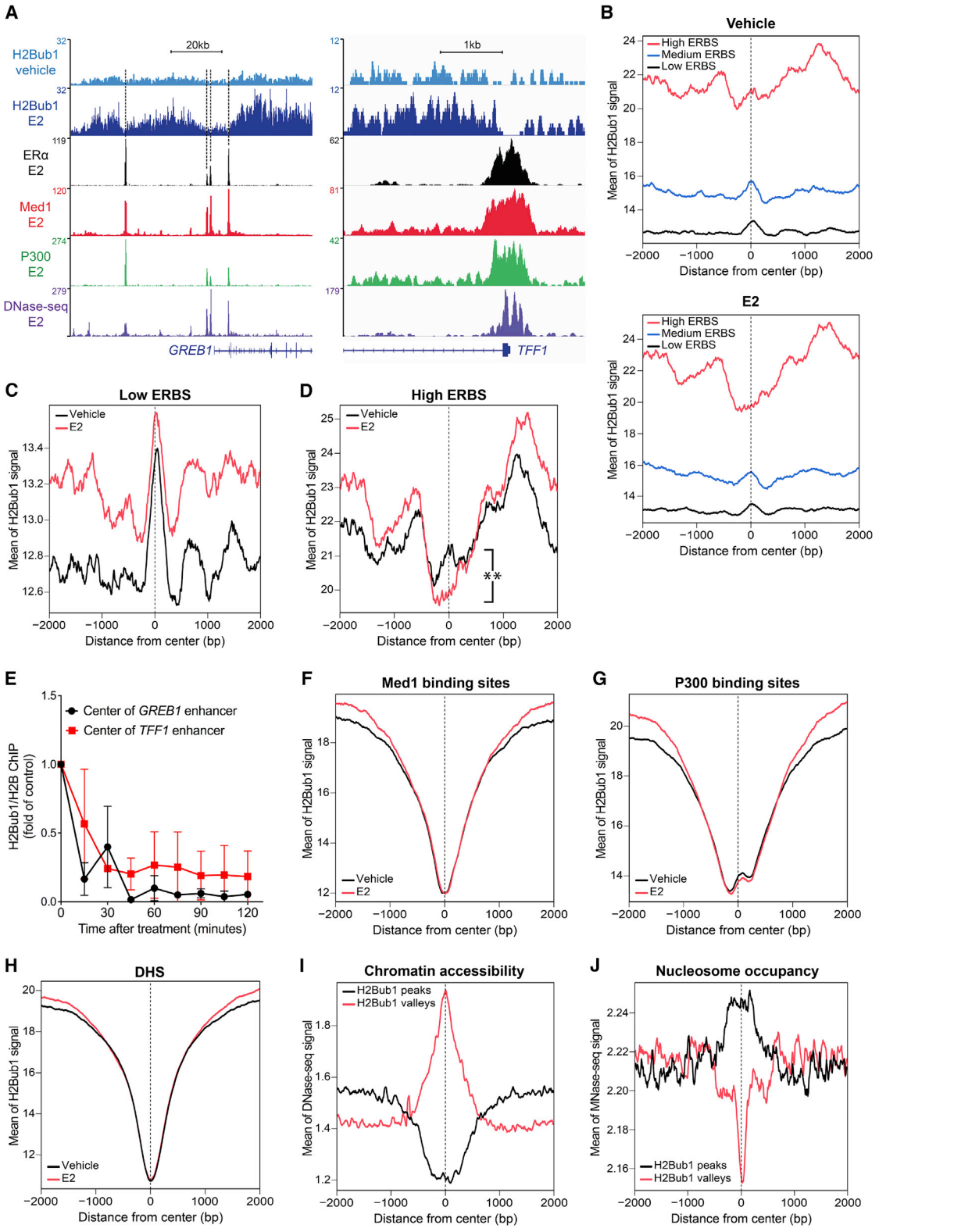

(legend on next page)

H2Bub1 Stabilizes the Association of H2A.Z with Inducible Enhancers

In the nucleosome, H2B forms dimers with H2A or H2A variants, of which H2A.Z is preferentially found at TSSs and enhancers (Jin et al., 2009; Dalvai et al., 2013; Brunelle et al., 2015). In agreement with this, we found that H2A.Z levels increase with the strength of the ERBS independent of any induction (Figures 4A and S4A). Interestingly, H2Bub1 forms valleys on H2A.Z binding sites, and the average signal of H2Bub1 positively correlates with the average signal of H2A.Z across strong ERBSs (Figures 4B and 4C). This suggests that H2Bub1 could be involved in the stabilization of H2A.Z in nucleosomes. In turn, an H2Bub1 valley at the center of H2A.Z binding sites could favor a destabilization of H2A.Z and promote chromatin accessibility. A time course experiment by ChIP of H2A.Z on the *GREB1* and *TFF1* enhancers confirmed that the levels of chromatin-associated H2A.Z decrease upon E2 induction, whereas the binding of ERα concomitantly increases (Figure 4D). Most importantly, upon impairing H2B monoubiquitination, H2A.Z strongly decreases on the *GREB1* and *TFF1* enhancers before and after E2 induction (Figures 4E and 4F). We concluded from these results that H2Bub1 specifically stabilizes H2A.Z on inducible enhancers because no striking effects were observed for H2A.Z on TSSs and for H2B itself (Figures S4B–S4G). For H2B, which would be evicted from enhancers along with H2A.Z, it must be mentioned that it could be reincorporated into nucleosomes with H2A (Papamichos-Chronakis et al., 2011).

To generate more direct evidence that it is indeed H2B monoubiquitination that stabilizes H2A.Z, we used the H2B monoubiquitination mutant K120R. Upon overexpressing the mutant compared with wild-type H2B, we observed a decrease of H2A.Z on the *GREB1* and *TFF1* enhancers (Figure 4G). Because we had shown that H2B monoubiquitination also regulates transfected reporter gene constructs (Figures 1B–1D), we wanted to provide further support for the stabilizing effect of H2Bub1 on H2A.Z with this system. An H2A.Z ChIP experiment with an ERα-dependent enhancer of a luciferase reporter showed that overexpression of RNF20 and RNF40 increases the stability of H2A.Z both without and with induction by E2 (Figure 4H). Lending further support to the validity of using transfected reporter plasmids, we confirmed with this construct that the induction by E2 decreases H2A.Z levels on the enhancer. The effect of H2B monoubiquitination on H2A.Z dynamics is general enough to be seen by co-immunoprecipitation because the overexpression of RNF20 and RNF40 increases the association of H2B with H2A.Z (Figure 4I). This suggests that H2B monoubiquitination affects the dynamics of association/dissociation of H2B with H2A.Z. H2Bub1 and H2A.Z have been linked to the transcription of antisense RNA (Zofall et al., 2009; Murray et al., 2015), which could arise from cryptic transcription initiation in gene bodies (Smolle and Workman, 2013). Indeed, impairing H2B monoubiquitination increases the production of antisense RNA in the *GREB1* and *TFF1* gene bodies (Figures 4J and 4K), indicating that H2Bub1 could play a role in controlling the H2A.Z dynamics to avoid nonspecific transcription initiation.

H2Bub1 Impairs the Interaction of INO80 with Inducible Enhancers

H2Bub1 could stabilize H2A.Z either by promoting its incorporation into nucleosomes or by blocking its eviction (Gerhold and Gasser, 2014). To gain insights into the proteins that could link H2A.Z dynamics with H2Bub1, we generated an in silico interactome of RNF20/40 based on data from public repositories (Figure 5A). This revealed an interaction between RNF40 and the chromatin remodeler INO80, already known to be involved in the eviction of H2A.Z (Papamichos-Chronakis et al., 2011), and ERα, as hinted at previously (Bedi et al., 2015). We first assessed whether the protein levels of INO80 are affected by the RNF20/40 knockdown. Although H2Bub1 levels decreased, INO80 levels remained unchanged both in MDA-MB134 and in HEK293T cells (Figure 5B). We then experimentally confirmed by several reciprocal co-immunoprecipitation experiments that INO80 interacts with RNF40 (Figure 5C) and that RNF40 interacts with ERα as well as RNA polymerase II (Figures S5A and S5B). Considering that RNF40 and RNF20 form a heterodimer, it was unexpected that we failed to co-immunoprecipitate RNF20 with INO80, ERα, and RNA polymerase II. At this point, we can only speculate that interactions of RNF20 with other proteins may be more labile, that the epitopes on which we relied are masked, or that the antibodies used interfered with these particular RNF20 complexes. We cannot formally exclude that the INO80-RNF40 complex is devoid of RNF20, but clarifying the functional relevance of this interaction and of the unusual prospect of RNF40 acting independently of RNF20 will require further investigation.

Figure 3. Monoubiquitination of Histone H2B Drops at Active Enhancers and Accessible Chromatin Regions

(A) Genomic profiles of H2Bub1, ERα, Med1, P300, and DNase I hypersensitivity (DNase-seq) over the 5′ regions of two E2-induced genes.

(B) Aggregate plot analyses of H2Bub1 in confidence level-based groups (high, medium, and low) of ERBSs in MCF-7 cells treated with vehicle alone (top) or E2 (bottom). High ERBS comprised 1,067 sites defined as having a confidence level ($-10 \times \log_{10}$ p value) in ERα ChIP-seq data of more than 150. Medium ERBSs (4,149 sites) are between 50 and 150, and low ERBS (10,558 sites) are less than 50.

(C and D) Aggregate plots of H2Bub1 associated with low ERBSs (C) or high ERBSs (D) (asterisks indicate a $p < 0.00001$ between vehicle and E2 conditions at the center).

(E) Kinetic analysis of H2Bub1 by ChIP-qPCR on the center of the *GREB1* (black circles) and *TFF1* (red squares) enhancers at different time points after E2 treatment of MDA-MB134 cells. For these ChIP experiments, MNase digestion was used instead of sonication, and the ChIP-qPCR values for H2Bub1 were normalized to those of H2B (H2Bub1/H2B). Values are represented as fold of control (untreated cells).

(F–H) Aggregate plot analyses of H2Bub1 at Med1 and P300 binding sites, and at DHSs with the indicated treatments.

(I and J) Aggregate plot analyses of DNase-seq (I, chromatin accessibility) and MNase-seq (J, nucleosome occupancy) signals over regions containing H2Bub1 peaks or valleys (defined and extracted as indicated in the Experimental Procedures). The reanalyses of ChIP-seq data were performed on the publicly available datasets with accession numbers GEO: GSE55921 (H2Bub1 and ERα), GSE60270 (Med1, P300), GSE33216 (DNase-seq), and GSE51097 (MNase-seq).

See also Figures S3A–S3J.

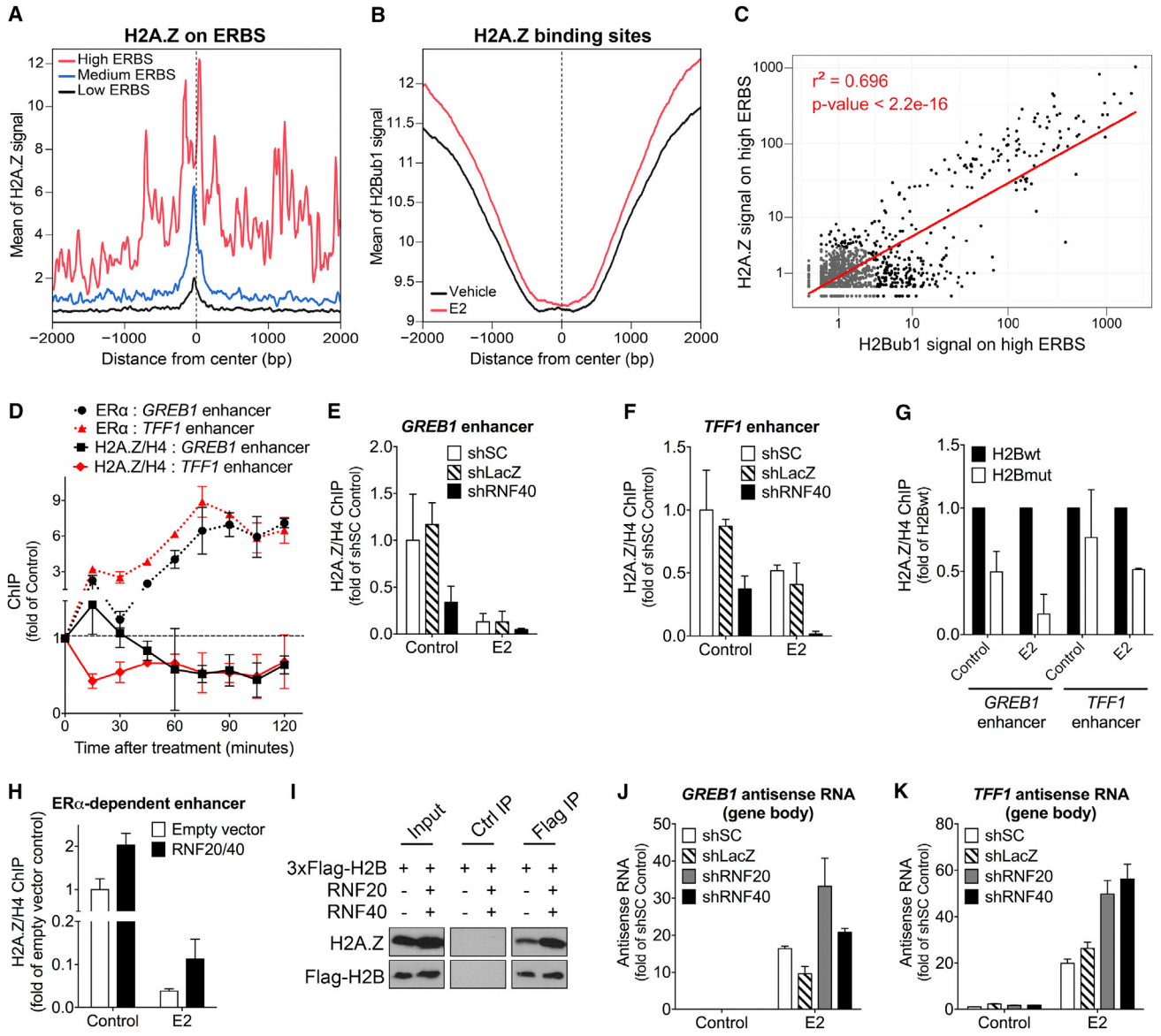

Figure 4. Histone H2B Monoubiquitination Controls the Occupancy of Histone H2A.Z at Active Enhancers

(A) Aggregate plot analysis of H2A.Z in confidence level-based groups (high, medium, and low) of ERBSs in MCF-7 cells treated with vehicle (see legend of Figure 3B).

(B) Aggregate plot of H2Bub1 at H2A.Z binding sites in MCF-7 cells with the indicated treatments.

(C) Scatterplot comparing the mean of the H2A.Z and H2Bub1 signals on high ERBSs. The coefficient of determination (r^2) and p value of the linear regression are indicated, and the dense area of dots was arbitrarily stained gray for clarity.

(D) ChIP-qPCR kinetics of ERα (dotted lines) and H2A.Z (full lines) on the *GREB1* (black) and *TFF1* (red) enhancers at different times after E2 treatment of MDA-MB134 cells. The ChIP-qPCR values of H2A.Z were normalized to those of H4 (H2A.Z/H4). Values are represented as fold of control (untreated cells).

(E and F) Effect of knockdown of RNF40 on the levels of H2A.Z at the *GREB1* (E) and *TFF1* (F) enhancers. MDA-MB134 cells were infected with the indicated shRNA constructs. H2A.Z/H4 ChIP-qPCR values are represented as fold of the shSC control.

(G) ChIP-qPCR of H2A.Z on the *GREB1* and *TFF1* enhancers in MDA-MB134 cells overexpressing either wild-type H2B (H2Bwt, black bars) or the H2B mutant K120/125R (H2Bmut, white bars). H2A.Z/H4 ChIP-qPCR values are represented as fold of H2Bwt.

(H) ChIP-qPCR of H2A.Z on the ERα-dependent enhancer of the transfected reporter plasmid upon overexpression of RNF20 and RNF40 in HEK293T cells. H2A.Z/H4 ChIP-qPCR values are represented as fold of empty vector control.

(I) Immunoblot of the immunoprecipitation of FLAG-tagged H2B (FLAG IP) expressed in HE293T cells with or without co-overexpression of RNF20/40. The blot was probed with antibodies to H2A.Z or FLAG. A control immunoprecipitation was performed in parallel with a control immunoglobulin G (IgG) (Ctrl IP).

(legend continued on next page)

INO80 appears to interact more strongly with ERα upon induction by E2 (Figure 5C). This suggested that INO80 could be part of transactivator complexes. The knockdown of INO80 reduced the stimulation of the endogenous *GREB1* and *TFF1* enhancers by RNF20/40 silencing (Figure 5D). Moreover, similar results were obtained with a transfected reporter gene assay. Knockdown of INO80 but not of the H2A.Z chaperone ANP32E (Obri et al., 2014) significantly reduced the stimulation of the E2-inducible enhancer by RNF20/40 silencing (Figures 5E and S5C). We also noticed that knockdown of INO80 by itself, but not of ANP32E, decreased the activity of the E2-inducible enhancer (Figure 5F). Consistent with the proposed antagonistic relationship between H2Bub1 and INO80 recruitment, the recruitment of INO80 is increased on the *GREB1* and *TFF1* enhancers upon E2 induction and further boosted by knockdown of RNF40 (Figure 5G). To ascertain that these effects are indeed due to changes in H2Bub1 levels, we demonstrated that the levels of INO80 on the *GREB1* and *TFF1* enhancers are increased upon overexpression of the monoubiquitination mutant of H2B (Figure 5H). Conversely, stimulation of H2B monoubiquitination by RNF20/40 overexpression decreases the recruitment of INO80 to an ERα-dependent enhancer, here in the context of a transfected reporter plasmid (Figure 5I). Finally, co-immunoprecipitation experiments demonstrated that overexpression of RNF20/40 decreases the interaction of INO80 with wild-type H2B (Figure 5J). Moreover, the interaction between INO80 and the monoubiquitination mutant of H2B is stronger than with wild-type H2B and insensitive to the overexpression of RNF20/40 (Figure 5J). Thus, H2Bub1 represses inducible enhancers by interfering with the recruitment of INO80 and the resulting eviction of H2A.Z.

DISCUSSION

We discovered a repressive role for the monoubiquitination of H2B for inducible transcription and suggested a molecular mechanism based on our study. In our model (Figure 6), the chromatin at inducible enhancers could be primed by the distribution and relative abundance of H2A.Z and H2Bub1 before induction. We discovered that both H2A.Z and H2Bub1 are enriched at regulatory sequences of induced genes (Figures 3B, 4A, and S4A) with a notable relative decrease in H2Bub1 at the very center of strong inducible enhancers, a feature we referred to as an H2Bub1 valley (Figures 3B, 3D, and S3A). We hypothesize that the eviction of the H2A.Z/H2B dimer by INO80 is impaired by H2Bub1 and, therefore, that the reduced levels of H2Bub1 at the center of inducible enhancers direct the eviction of H2A.Z/H2B to this location to maintain a defined region accessible to transcription factors and their coactivators such as Med1 and P300. Upon induction, the levels of H2Bub1 decrease further at the center of inducible enhancers, whereas they increase on both sides surrounding these enhancers (Figure 3D). An H2Bub1 deubiquitinase (DUB) such as USP22, which is associated with the coactivator complex SAGA (Zhang et al., 2008), or the proteasome-associated DUB Uch37, which can be recruited by INO80 itself (Yao et al., 2008), could be responsible for removing the H2Bub1 mark from the center of the induced enhancers. Because of the stabilization of H2A.Z-containing nucleosomes by H2Bub1 through the stabilization of H2A.Z/H2B dimers, the increase of H2Bub1 on both sides of the induced enhancer could prevent the spreading of accessible chromatin. Because INO80 interacts with active transcription factor complexes (Cai et al., 2007; Figure 5C), it is conceivable that it also removes H2A.Z/H2B dimers in the immediate vicinity to favor the recruitment of additional transcription factors. Moreover, this process could be facilitated by the INO80-associated DUB Uch37. This could contribute to forming the complex transcription factor hubs characterized previously for nuclear receptors and other transcription factors (see, for example, Liu et al., 2014).

There are several possibilities to explain the stabilization of H2A.Z in the chromatin of strong inducible enhancers by H2Bub1. Like histones, ubiquitin is a lysine-rich protein, and, therefore, the stabilizing effect of H2Bub1 on the nucleosome could be mediated by an increased affinity for DNA (Chandrasekharan et al., 2009). This could strengthen the contact between the H2B-H2A.Z dimer and DNA and increase the energy barrier for its eviction by the ATP-dependent chromatin remodeler INO80. An alternative but not mutually exclusive explanation rests on our finding that H2Bub1 inhibits the binding of INO80 to strong inducible enhancers (Figure 5G). It is conceivable that the coupling of an ubiquitin molecule to H2B could impair the interaction of INO80 with the nucleosome because of steric hindrance. Indeed, the conjugation of an ubiquitin molecule to H2B is a very bulky modification of the core of the protein that represents half of its mass. This second explanation is supported by our finding that the interaction of INO80 with H2B is decreased by the monoubiquitination of H2B (Figure 5J) and by the detailed interaction map of the nucleosome with the INO80 complex, recently determined by mass spectrometry (Tosi et al., 2013). Some interactions between H2B of *Drosophila melanogaster* and several components of the INO80 complex were mapped to K118, the H2B ubiquitination site in this organism. The juxtaposition of the conjugated ubiquitin with the interaction site could prevent the binding of essential components of the INO80 complex to the nucleosome and, thereby, the INO80-mediated eviction of H2B/H2A.Z dimers. Ultimately, reconstitution experiments with chemically ubiquitylated H2B and other purified components (Zhou et al., 2016) could help to dissect the molecular details of this remodeling reaction.

One of the findings that appears confusing at first sight relates to the global distribution of H2Bub1 on inducible enhancers. We found that H2Bub1 and H2A.Z levels are positively correlated on strong inducible enhancers (Figure 4C) and that their respective abundances increase proportionally with the strength of the

(J and K) Effect of knockdown of RNF20/40 on antisense RNAs over the *GREB1* (J) and *TFF1* (K) gene bodies. MDA-MB134 cells were infected with the indicated shRNA constructs. Antisense RNA levels are represented as fold of the shSC control.

An empty vector was transfected as a negative control for RNF20/40 overexpression experiments (H and I). Both shSC- and shLacZ-infected MDA-MB134 cells were used as negative controls (E, F, J, and K). Datasets GEO: GSE55921 (H2Bub1 and ERα) and GSE57436 (H2A.Z) were used (A–C).

The bar graphs show averages of several independent experiments with technical replicates and the errors of the means. See also Figures S4A–S4G.

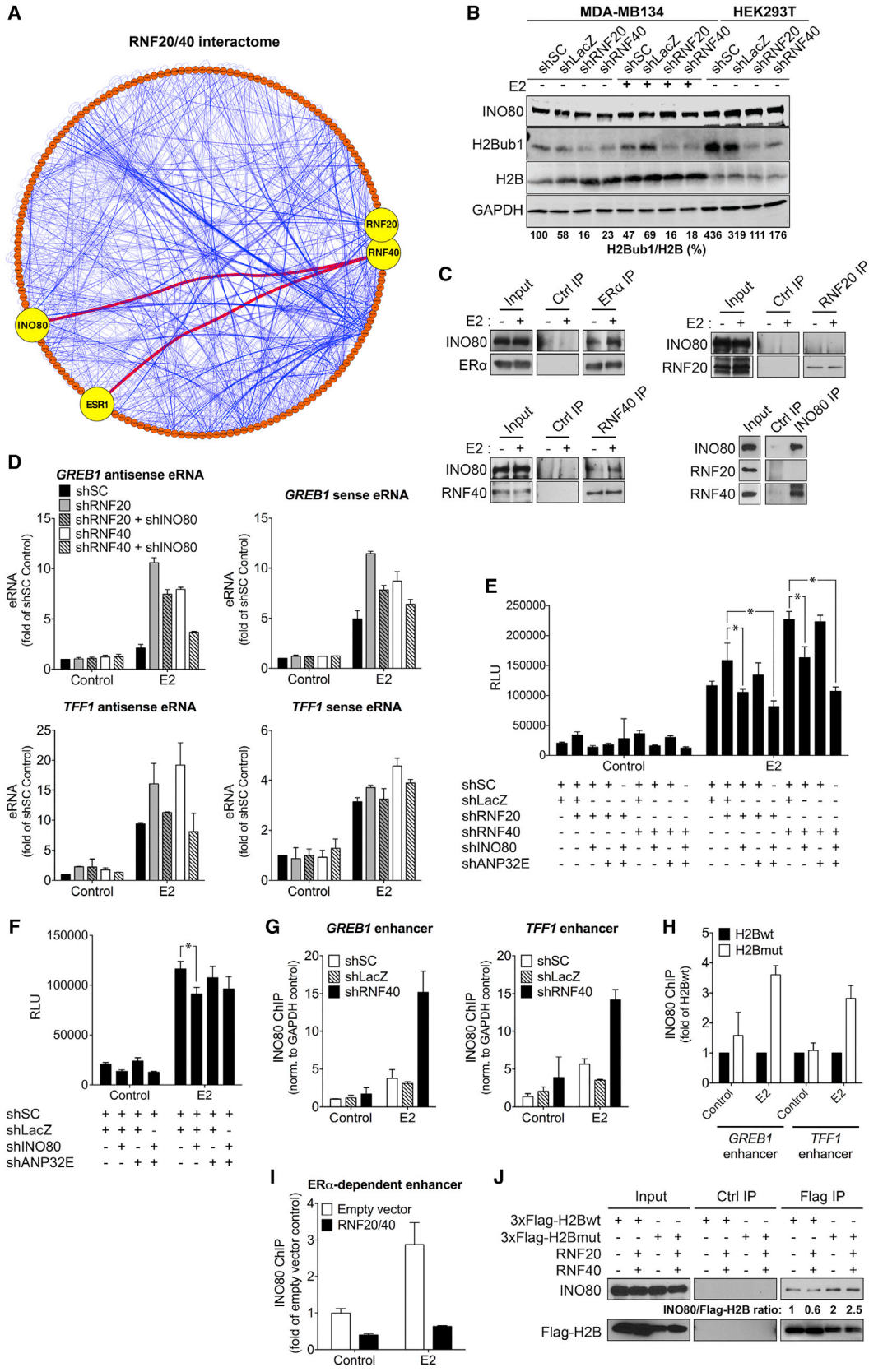

(legend on next page)

inducible enhancers (Figures 3B, 4A, and S4A). This suggests that proteins responsible for the H2Bub1 mark could somehow be functionally linked to the proteins involved in H2A.Z dynamics. Indeed, we found that INO80 interacts with RNF40 (Figure 5C), but there could be additional interactions between other players of the H2Bub1 and H2A.Z pathways. Identifying these interactions and determining their functional consequences could help to explain the functional relationship that may link the distribution of H2Bub1 with H2A.Z and, more generally, with the strength of the inducible enhancers.

By analogy to the increase in H2Bub1 levels within the gene bodies that arises from transcriptional elongation by RNA polymerase II (Minsky et al., 2008; Fuchs et al., 2014), we hypothesize that the transcription of eRNAs on both sides of the enhancer could explain the observed increase of H2Bub1 levels. In contrast, the observed decrease of H2Bub1 levels at the center of activated inducible enhancers could be due to deubiquitination by the SAGA complex. This speculation is supported by the characterization of USP22, the deubiquitinase subunit of SAGA, as a coactivator of the androgen receptor, another member of the superfamily of nuclear receptors (Zhao et al., 2008). Since H2Bub1 valleys are found exactly where transcriptional activators bind (Figures 3F and 3G), this suggests that, upon induction, H2Bub1 is further deubiquitinated, where H2A.Z has to be evicted by INO80 to allow additional transcriptional activators to gain access to the DNA. However, because there are already H2Bub1 valleys at the center of inducible enhancers before induction, albeit less pronounced than after induction, this suggests that additional mechanisms are involved in setting up the initial H2Bub1 distribution.

We demonstrated that INO80 interacts with ERα (Figure 5C) and, presumably, other transcriptional activators and that it is preferentially recruited to activated inducible enhancers (Figure 5G). Consistent with our results showing a time-dependent reduction of H2A.Z at inducible enhancers after activation (Figure 4D), this suggests that the eviction of H2A.Z by INO80 is necessary for inducible enhancer activation by the recruitment of transcriptional activators. This is in agreement with several studies that had highlighted a role of INO80 as a transcriptional coactivator (Cai et al., 2007; Li et al., 2012; Wang et al., 2014). Thus, this complements the role of INO80 in promoting the turnover of H2A.Z-containing nucleosomes (Yen et al., 2013) and its contribution to their disassembly following gene activation (Papamichos-Chronakis et al., 2011; Yen et al., 2013).

The genomic distribution of H2A.Z has been demonstrated to be controlled by Facilitates Chromatin Transcription (FACT) to avoid its misincorporation into chromatin, which would contribute to the formation of cryptic initiation sites (Jeronimo et al., 2015). In turn, we showed that the reduction of H2Bub1 leads to an increase in cryptic transcripts during target gene activation (Figures 4J and 4K). These results suggest that a tight spatial control of the distribution of H2A.Z may be exerted by FACT and H2Bub1 to avoid the generation of cryptic sites and to prevent transcription initiation at these sites, respectively. Moreover, because H2Bub1 and FACT were described to function cooperatively in transcriptional elongation (Pavri et al., 2006), they may also control the distribution and dynamics of H2A.Z in a cooperative manner.

Although H2Bub1 has been considered to be primarily a regulator of transcriptional elongation, we have demonstrated that H2Bub1 plays an essential role for the regulation of inducible enhancers by acting as a gatekeeper of H2A.Z eviction. In the future, the interplay between H2Bub1 and H2A.Z should be studied in more detail to determine how general it is for inducible enhancers and whether it is restricted to inducible enhancers or at play at other regulatory elements in the genome as well. The mechanism we have highlighted should also prompt studies of the activator role of H2B deubiquitinases for transcription initiation and of additional aspects of the architecture of inducible enhancers and their regulation.

Figure 5. Recruitment of the Histone H2A.Z Remodeler INO80 to Inducible Enhancers Is Impaired by H2B Monoubiquitination

(A) Combined interactome of RNF20 and RNF40 generated with Cytoscape using the PPiMapBuilder plug-in. Two interactors of interest are highlighted in yellow, and interactions between them are shown in red. Note that ESR1 is the official name of ERα.

(B) Knockdown of RNF20 or RNF40 affects H2Bub1 but not INO80 levels. Protein extracts were made from MDA-MB134 cells and HEK293T cells infected with the indicated shRNA constructs. Immunoblotting was performed for INO80, H2Bub1, H2B, and GAPDH, and H2Bub1 levels relative to H2B levels were determined with the software ImageJ.

(C) The INO80 interaction with ERα and RNF40 is stimulated by E2. Shown is immunoprecipitation of ERα, RNF20, RNF40, or INO80 from extracts of MDA-MB134 cells treated with vehicle (−) or E2 (+, where indicated), followed by immunoblotting. A control immunoprecipitation was performed in parallel with a control IgG.

(D) Quantification by qPCR of the eRNAs of the *GREB1* and *TFF1* enhancers in MDA-MB134 cells infected with the indicated shRNA constructs. eRNA levels are relative to the shSC control condition.

(E and F) Luciferase reporter gene assays of an ERα-dependent enhancer in HEK293T cells infected with the indicated shRNA constructs. Relevant statistically significant values are highlighted by asterisks (*$p < 0.05$).

(G) ChIP-qPCR of INO80 on the *GREB1* and *TFF1* enhancers with MDA-MB134 cells infected with the indicated shRNA constructs. INO80 ChIP-qPCR values are standardized to the GAPDH internal standard.

(H) ChIP-qPCR of INO80 on the *GREB1* and *TFF1* enhancers with MDA-MB134 cells overexpressing either wild-type H2B (H2Bwt, black bars) or the H2B mutant K120/125R (H2Bmut, white bars). INO80 ChIP-qPCR values are represented as fold of H2Bwt.

(I) ChIP-qPCR of INO80 on the ERα-dependent enhancer of the transfected reporter plasmid upon overexpression of RNF20/40 in HEK293T cells. INO80 ChIP-qPCR values are represented as fold of empty vector control.

(J) Immunoprecipitation of FLAG-tagged H2B (FLAG IP) followed by immunoblotting of INO80 or FLAG performed with extracts of HEK293T cells transfected with either FLAG-tagged H2Bwt or H2Bmut and overexpressing RNF20/40. Co-immunoprecipitated INO80 levels were normalized to total INO80 levels and expressed as a ratio relative to immunoprecipitated FLAG-H2B. A control immunoprecipitation was performed in parallel with a control IgG (Ctrl IP).

An empty vector was transfected as a negative control for RNF20/40 overexpression experiments (I and J). shSC- and shLacZ-infected cells were used as negative controls (B and D–G). The bar graphs show averages of several independent experiments with technical replicates and the errors of the means. See also Figures S5A–S5C.

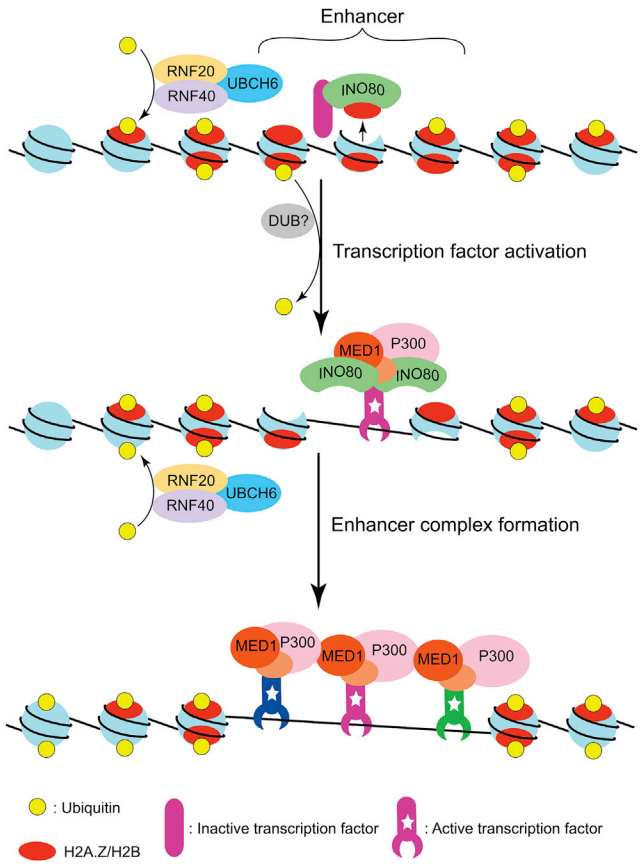

Figure 6. Schematic of the Model

It depicts the proposed mechanism of the regulation of inducible enhancers by H2B monoubiquitination through the inhibition of the eviction of H2A.Z by INO80.

EXPERIMENTAL PROCEDURES

See the Supplemental Experimental Procedures for additional details.

Cell Culture

Induction of ERα was done with 100 nM 17β-estradiol (Sigma-Aldrich), of GR with 100 nM dexamethasone (Sigma-Aldrich), and of PR with 100 nM progesterone (Sigma-Aldrich). Transfections were performed with polyethylenimine (PEI) transfection reagent mixed with DNA at a DNA:PEI ratio of 1:3. Knockdowns were generated by infection with lentiviruses expressing specific shRNA against each targeted mRNA.

Luciferase Assays

Cells were lysed using passive lysis buffer (Promega) and firefly luciferase, and *Renilla* luciferase activities were measured in cell lysates with the Dual-Luciferase kit (Promega) with a bioluminescence plate reader. *Renilla* luciferase activity was used as a transfection control.

Reverse Transcription and qPCR

For the quantification of antisense RNA, specific primers instead of random primers were used for reverse transcription (Table S1). In qPCR experiments, RNA levels were standardized with *GAPDH* as the internal standard.

ChIP

The protocol for ChIP experiments was the one described by Schmidt et al. (2009). ChIP values were standardized with internal controls (the *c-MYC* intron for the ChIP of ERα and FOXA1 or the *GAPDH* coding region for the ChIP of H2A.Z, H4, H2Bub1, H2B, and INO80) and normalized with the input values.

ChIP-Seq Data Re-analyses and Interactome

The following ChIP-seq datasets, available publicly on the NCBI server, were used GEO: GSE55921 (H2Bub1 and ERα) (Nagarajan et al., 2014), GSE60270 (Med1 and P300) (Liu et al., 2014), GSE33216 (DNase-seq) (He et al., 2012), GSE51097 (MNase-seq) (Shimbo et al., 2013), GSE23701 (H3K9me3 and H3K27me3) (Joseph et al., 2010), GSE40129 (H3K27ac) (Theodorou et al., 2013), GSE33213 (CTCF, Encyclopedia of DNA Elements [ENCODE]), and GSE57436 (H2A.Z) (Brunelle et al., 2015). Sequence Read Archive (SRA) files from each dataset were downloaded from the NCBI server, converted into fastq files, and mapped to the human reference genome hg19 with bwa mem. Visualization of ChIP-seq profiles was performed with the Integrative Genomics Viewer (version 2.3.67). Peak calling was carried out by using the model-based analysis of ChIP-seq (MACS) tool from the Galaxy framework. ERBSs were separated into three groups (high, medium, and low) by using R based on the confidence level ($-10 \times \log_{10}$ p value) of the peak center of ERBSs. The high, medium, and low groups correspond to ERBSs with confidence levels of more than 150, 50–150, and less than 50, respectively. H2Bub1 valleys were defined as gaps of less than 50 kb between H2Bub1 peaks, and they were extracted with R. Aggregation plots were done with the Cistrome tool (Galaxy instance). The means of the H2A.Z and H2Bub1 signals on high ERBSs were determined by mapping the mean coverage of H2A.Z and H2Bub1 on high ERBS gaps with bedtools map. The scatterplot, linear regression, and calculations of the coefficient of determination (r^2) and p value were done with R. The combined interactome of RNF20 and RNF40 was obtained with the PPiMapBuilder plug-in (https://github.com/PPiMapBuilder/PPiMapBuilder, developed based on a previous study by Echeverría et al., 2011) of the Cytoscape freeware on all of the available interactome databases and organisms proposed by the plug-in.

Statistical Analyses

The bar graphs show averages of several independent experiments with technical replicates and the errors of the means. Statistical significance was determined with Student's t test.

SUPPLEMENTAL INFORMATION

Supplemental Information includes Supplemental Experimental Procedures, five figures, and two tables and can be found with this article online at http://dx.doi.org/10.1016/j.molcel.2016.08.034.

AUTHOR CONTRIBUTIONS

G.S. and D.P. designed the experiments. G.S. performed the vast majority of the experiments. M.A.B. performed several experiments, and D.P.P. made the initial discovery of Bre1/Rad6 in a yeast screen. N.H. contributed to the bioinformatic analyses. G.S., M.A.B., D.P.P., N.H., and D.P. analyzed the data. G.S. and D.P. wrote the paper. M.A.B. and D.P.P. contributed equally to this work.

ACKNOWLEDGMENTS

We are grateful to Pierre Frey and Kamilla Malinowska for their early efforts on this project, Lilia Bernasconi for technical assistance at the beginning of the project, Julien Soudet and Joan Conaway for helpful discussions, Pierre Dupuis and colleagues for the PPiMapBuilder plug-in, and numerous other colleagues for their gifts of reagents. This work was supported by the Canton de Genève, the Swiss National Science Foundation, and the Fondation Medic.

Received: April 15, 2016
Revised: July 22, 2016
Accepted: August 26, 2016
Published: September 29, 2016

REFERENCES

Batta, K., Zhang, Z., Yen, K., Goffman, D.B., and Pugh, B.F. (2011). Genome-wide function of H2B ubiquitylation in promoter and genic regions. Genes Dev. *25*, 2254–2265.

Bedi, U., Scheel, A.H., Hennion, M., Begus-Nahrmann, Y., Rüschoff, J., and Johnsen, S.A. (2015). SUPT6H controls estrogen receptor activity and cellular differentiation by multiple epigenomic mechanisms. Oncogene *34*, 465–473.

Bennesch, M.A., and Picard, D. (2015). Minireview: Tipping the balance: ligand-independent activation of steroid receptors. Mol. Endocrinol. *29*, 349–363.

Brunelle, M., Nordell Markovits, A., Rodrigue, S., Lupien, M., Jacques, P.E., and Gévry, N. (2015). The histone variant H2A.Z is an important regulator of enhancer activity. Nucleic Acids Res. *43*, 9742–9756.

Cai, Y., Jin, J., Yao, T., Gottschalk, A.J., Swanson, S.K., Wu, S., Shi, Y., Washburn, M.P., Florens, L., Conaway, R.C., and Conaway, J.W. (2007). YY1 functions with INO80 to activate transcription. Nat. Struct. Mol. Biol. *14*, 872–874.

Chandrasekharan, M.B., Huang, F., and Sun, Z.W. (2009). Ubiquitination of histone H2B regulates chromatin dynamics by enhancing nucleosome stability. Proc. Natl. Acad. Sci. USA *106*, 16686–16691.

Chauhan, S., and Boyd, D.D. (2012). Regulation of u-PAR gene expression by H2A.Z is modulated by the MEK-ERK/AP-1 pathway. Nucleic Acids Res. *40*, 600–613.

Dalvai, M., Fleury, L., Bellucci, L., Kocanova, S., and Bystricky, K. (2013). TIP48/Reptin and H2A.Z requirement for initiating chromatin remodeling in estrogen-activated transcription. PLoS Genet. *9*, e1003387.

Echeverría, P.C., Bernthaler, A., Dupuis, P., Mayer, B., and Picard, D. (2011). An interaction network predicted from public data as a discovery tool: application to the Hsp90 molecular chaperone machine. PLoS ONE *6*, e26044.

Fleming, A.B., Kao, C.F., Hillyer, C., Pikaart, M., and Osley, M.A. (2008). H2B ubiquitylation plays a role in nucleosome dynamics during transcription elongation. Mol. Cell *31*, 57–66.

Fuchs, G., Shema, E., Vesterman, R., Kotler, E., Wolchinsky, Z., Wilder, S., Golomb, L., Pribluda, A., Zhang, F., Haj-Yahya, M., et al. (2012). RNF20 and USP44 regulate stem cell differentiation by modulating H2B monoubiquitylation. Mol. Cell *46*, 662–673.

Fuchs, G., Hollander, D., Voichek, Y., Ast, G., and Oren, M. (2014). Cotranscriptional histone H2B monoubiquitylation is tightly coupled with RNA polymerase II elongation rate. Genome Res. *24*, 1572–1583.

Gerhold, C.B., and Gasser, S.M. (2014). INO80 and SWR complexes: relating structure to function in chromatin remodeling. Trends Cell Biol. *24*, 619–631.

Gévry, N., Hardy, S., Jacques, P.E., Laflamme, L., Svotelis, A., Robert, F., and Gaudreau, L. (2009). Histone H2A.Z is essential for estrogen receptor signaling. Genes Dev. *23*, 1522–1533.

He, H.H., Meyer, C.A., Chen, M.W., Jordan, V.C., Brown, M., and Liu, X.S. (2012). Differential DNase I hypersensitivity reveals factor-dependent chromatin dynamics. Genome Res. *22*, 1015–1025.

Hurtado, A., Holmes, K.A., Ross-Innes, C.S., Schmidt, D., and Carroll, J.S. (2011). FOXA1 is a key determinant of estrogen receptor function and endocrine response. Nat. Genet. *43*, 27–33.

Jeronimo, C., Watanabe, S., Kaplan, C.D., Peterson, C.L., and Robert, F. (2015). The histone chaperones FACT and Spt6 restrict H2A.Z from intragenic locations. Mol. Cell *58*, 1113–1123.

Jin, C., Zang, C., Wei, G., Cui, K., Peng, W., Zhao, K., and Felsenfeld, G. (2009). H3.3/H2A.Z double variant-containing nucleosomes mark 'nucleosome-free regions' of active promoters and other regulatory regions. Nat. Genet. *41*, 941–945.

Joseph, R., Orlov, Y.L., Huss, M., Sun, W., Kong, S.L., Ukil, L., Pan, Y.F., Li, G., Lim, M., Thomsen, J.S., et al. (2010). Integrative model of genomic factors for determining binding site selection by estrogen receptor-α. Mol. Syst. Biol. *6*, 456.

Karpiuk, O., Najafova, Z., Kramer, F., Hennion, M., Galonska, C., König, A., Snaidero, N., Vogel, T., Shchebet, A., Begus-Nahrmann, Y., et al. (2012). The histone H2B monoubiquitination regulatory pathway is required for differentiation of multipotent stem cells. Mol. Cell *46*, 705–713.

Li, Z., Gadue, P., Chen, K., Jiao, Y., Tuteja, G., Schug, J., Li, W., and Kaestner, K.H. (2012). Foxa2 and H2A.Z mediate nucleosome depletion during embryonic stem cell differentiation. Cell *151*, 1608–1616.

Li, W., Notani, D., Ma, Q., Tanasa, B., Nunez, E., Chen, A.Y., Merkurjev, D., Zhang, J., Ohgi, K., Song, X., et al. (2013). Functional roles of enhancer RNAs for oestrogen-dependent transcriptional activation. Nature *498*, 516–520.

Liu, Z., Merkurjev, D., Yang, F., Li, W., Oh, S., Friedman, M.J., Song, X., Zhang, F., Ma, Q., Ohgi, K.A., et al. (2014). Enhancer activation requires trans-recruitment of a mega transcription factor complex. Cell *159*, 358–373.

Materne, P., Vázquez, E., Sánchez, M., Yague-Sanz, C., Anandhakumar, J., Migeot, V., Antequera, F., and Hermand, D. (2016). Histone H2B ubiquitylation represses gametogenesis by opposing RSC-dependent chromatin remodeling at the ste11 master regulator locus. eLife *5*, e13500.

Minsky, N., Shema, E., Field, Y., Schuster, M., Segal, E., and Oren, M. (2008). Monoubiquitinated H2B is associated with the transcribed region of highly expressed genes in human cells. Nat. Cell Biol. *10*, 483–488.

Murray, S.C., Haenni, S., Howe, F.S., Fischl, H., Chocian, K., Nair, A., and Mellor, J. (2015). Sense and antisense transcription are associated with distinct chromatin architectures across genes. Nucleic Acids Res. *43*, 7823–7837.

Nagarajan, S., Hossan, T., Alawi, M., Najafova, Z., Indenbirken, D., Bedi, U., Taipaleenmäki, H., Ben-Batalla, I., Scheller, M., Loges, S., et al. (2014). Bromodomain protein BRD4 is required for estrogen receptor-dependent enhancer activation and gene transcription. Cell Rep. *8*, 460–469.

Obri, A., Ouararhni, K., Papin, C., Diebold, M.L., Padmanabhan, K., Marek, M., Stoll, I., Roy, L., Reilly, P.T., Mak, T.W., et al. (2014). ANP32E is a histone chaperone that removes H2A.Z from chromatin. Nature *505*, 648–653.

Papamichos-Chronakis, M., Watanabe, S., Rando, O.J., and Peterson, C.L. (2011). Global regulation of H2A.Z localization by the INO80 chromatin-remodeling enzyme is essential for genome integrity. Cell *144*, 200–213.

Pavri, R., Zhu, B., Li, G., Trojer, P., Mandal, S., Shilatifard, A., and Reinberg, D. (2006). Histone H2B monoubiquitination functions cooperatively with FACT to regulate elongation by RNA polymerase II. Cell *125*, 703–717.

Prenzel, T., Begus-Nahrmann, Y., Kramer, F., Hennion, M., Hsu, C., Gorsler, T., Hintermair, C., Eick, D., Kremmer, E., Simons, M., et al. (2011). Estrogen-dependent gene transcription in human breast cancer cells relies upon proteasome-dependent monoubiquitination of histone H2B. Cancer Res. *71*, 5739–5753.

Schmidt, D., Wilson, M.D., Spyrou, C., Brown, G.D., Hadfield, J., and Odom, D.T. (2009). ChIP-seq: using high-throughput sequencing to discover protein-DNA interactions. Methods *48*, 240–248.

Shema, E., Tirosh, I., Aylon, Y., Huang, J., Ye, C., Moskovits, N., Raver-Shapira, N., Minsky, N., Pirngruber, J., Tarcic, G., et al. (2008). The histone H2B-specific ubiquitin ligase RNF20/hBRE1 acts as a putative tumor suppressor through selective regulation of gene expression. Genes Dev. *22*, 2664–2676.

Shimbo, T., Du, Y., Grimm, S.A., Dhasarathy, A., Mav, D., Shah, R.R., Shi, H., and Wade, P.A. (2013). MBD3 localizes at promoters, gene bodies and enhancers of active genes. PLoS Genet. *9*, e1004028.

Shlyueva, D., Stampfel, G., and Stark, A. (2014). Transcriptional enhancers: from properties to genome-wide predictions. Nat. Rev. Genet. *15*, 272–286.

Smolle, M., and Workman, J.L. (2013). Transcription-associated histone modifications and cryptic transcription. Biochim. Biophys. Acta *1829*, 84–97.

Tarcic, O., Pateras, I.S., Cooks, T., Shema, E., Kanterman, J., Ashkenazi, H., Boocholez, H., Hubert, A., Rotkopf, R., Baniyash, M., et al. (2016). RNF20 links histone H2B ubiquitylation with inflammation and inflammation-associated cancer. Cell Rep. *14*, 1462–1476.

Teves, S.S., Weber, C.M., and Henikoff, S. (2014). Transcribing through the nucleosome. Trends Biochem. Sci. *39*, 577–586.

Theodorou, V., Stark, R., Menon, S., and Carroll, J.S. (2013). GATA3 acts upstream of FOXA1 in mediating ESR1 binding by shaping enhancer accessibility. Genome Res. *23*, 12–22.

Tosi, A., Haas, C., Herzog, F., Gilmozzi, A., Berninghausen, O., Ungewickell, C., Gerhold, C.B., Lakomek, K., Aebersold, R., Beckmann, R., and Hopfner, K.P. (2013). Structure and subunit topology of the INO80 chromatin remodeler and its nucleosome complex. Cell *154*, 1207–1219.

Venkatesh, S., and Workman, J.L. (2015). Histone exchange, chromatin structure and the regulation of transcription. Nat. Rev. Mol. Cell Biol. *16*, 178–189.

Wang, L., Du, Y., Ward, J.M., Shimbo, T., Lackford, B., Zheng, X., Miao, Y.L., Zhou, B., Han, L., Fargo, D.C., et al. (2014). INO80 facilitates pluripotency gene activation in embryonic stem cell self-renewal, reprogramming, and blastocyst development. Cell Stem Cell *14*, 575–591.

Watanabe, S., Radman-Livaja, M., Rando, O.J., and Peterson, C.L. (2013). A histone acetylation switch regulates H2A.Z deposition by the SWR-C remodeling enzyme. Science *340*, 195–199.

Weake, V.M., and Workman, J.L. (2008). Histone ubiquitination: triggering gene activity. Mol. Cell *29*, 653–663.

Yao, T., Song, L., Jin, J., Cai, Y., Takahashi, H., Swanson, S.K., Washburn, M.P., Florens, L., Conaway, R.C., Cohen, R.E., and Conaway, J.W. (2008). Distinct modes of regulation of the Uch37 deubiquitinating enzyme in the proteasome and in the Ino80 chromatin-remodeling complex. Mol. Cell *31*, 909–917.

Yen, K., Vinayachandran, V., and Pugh, B.F. (2013). SWR-C and INO80 chromatin remodelers recognize nucleosome-free regions near +1 nucleosomes. Cell *154*, 1246–1256.

Zentner, G.E., and Henikoff, S. (2013). Regulation of nucleosome dynamics by histone modifications. Nat. Struct. Mol. Biol. *20*, 259–266.

Zhang, X.Y., Varthi, M., Sykes, S.M., Phillips, C., Warzecha, C., Zhu, W., Wyce, A., Thorne, A.W., Berger, S.L., and McMahon, S.B. (2008). The putative cancer stem cell marker USP22 is a subunit of the human SAGA complex required for activated transcription and cell-cycle progression. Mol. Cell *29*, 102–111.

Zhao, Y., Lang, G., Ito, S., Bonnet, J., Metzger, E., Sawatsubashi, S., Suzuki, E., Le Guezennec, X., Stunnenberg, H.G., Krasnov, A., et al. (2008). A TFTC/STAGA module mediates histone H2A and H2B deubiquitination, coactivates nuclear receptors, and counteracts heterochromatin silencing. Mol. Cell *29*, 92–101.

Zhou, L., Holt, M.T., Ohashi, N., Zhao, A., Müller, M.M., Wang, B., and Muir, T.W. (2016). Evidence that ubiquitylated H2B corrals hDot1L on the nucleosomal surface to induce H3K79 methylation. Nat. Commun. *7*, 10589.

Zhu, B., Zheng, Y., Pham, A.D., Mandal, S.S., Erdjument-Bromage, H., Tempst, P., and Reinberg, D. (2005). Monoubiquitination of human histone H2B: the factors involved and their roles in HOX gene regulation. Mol. Cell *20*, 601–611.

Zofall, M., Fischer, T., Zhang, K., Zhou, M., Cui, B., Veenstra, T.D., and Grewal, S.I. (2009). Histone H2A.Z cooperates with RNAi and heterochromatin factors to suppress antisense RNAs. Nature *461*, 419–422.